Acta Oceanol. Sin., 2025, Vol. 44, No. 4, P. 48–62
https://doi.org/10.1007/s13131-024-2457-z

Sources and distribution characteristics of chromophoric dissolved organic matter in the Cosmonaut Sea and the Cooperation Sea, Antarctica

Ji Hu[1], Siyou Xue[1, 2], Bin Zhou[3], Jun Zhao[1], Dong Li[1], Gaojing Fan[4], Disong Yang[5, 6], Leilei Zhang[7], Haifeng Zhang[1], Peisong Yu[1], Cai Zhang[1], Xufeng Yang[1], Changfeng Zhu[1], Weiping Sun[1], Jianming Pan[1*]

[1] Key Laboratory of Marine Ecosystem Dynamics, Second Institute of Oceanography, Ministry of Natural Resources, Hangzhou 310012, China
[2] College of Ocean and Earth Sciences, Xiamen University, Xiamen 361102, China
[3] North China Sea Survey Center, Ministry of Natural Resources, Qingdao 2660611, China
[4] Polar Research Institute of China, Shanghai 201209, China
[5] North China Sea Ecological Center of the Ministry of Natural Resources, Qingdao 266033, China
[6] Key Laboratory of Ecological Prewarning, Protection and Restoration of Bohai Sea, Ministry of Natural Resources, Qingdao 266033, China
[7] Dalian Marine Center, Ministry of Natural Resources, Dalian 116023, China

Received 15 October 2024; accepted 8 February 2025
© Chinese Society for Oceanography and Springer-Verlag GmbH Germany, part of Springer Nature 2025

Abstract

Dissolved organic carbon (DOC) constitutes the largest organic carbon reservoir in the ocean and plays a vital role in the oceanic carbon cycle. However, research on DOC in Antarctica has been limited, largely due to difficulties in sample collection. In this study, we investigate chromophoric dissolved organic matter (CDOM) in the Cosmonaut Sea and Cooperation Sea, Antarctica. The relative abundances of CDOM, as indicated by the absorption coefficient at 254 nm (a_{254}), exhibit significant variability, ranging from 1.29 m^{-1} to 8.37 m^{-1}. The diatom species B is the primary contributor to CDOM in the region influenced by the Antarctic slope current. Using excitation-emission matrix fluorescence spectroscopy coupled with parallel factor analysis (EEM-PARAFAC), we identify three fluorescent components: one protein-like component (C1) and two humic-like components (C2 and C3). Our findings indicate that strong microbial activity in the euphotic zones of the Cosmonaut Sea and Cooperation Sea serves as a primary pathway for the removal of protein-like substances while also acting as a significant source of humic-like substances. Microbial degradation likely accounts for the decoupling of the vertical distribution of DOC and phytoplankton. Furthermore, the intrusion of modified circumpolar deep water (mCDW) into the euphotic zones of open ocean areas influences the distribution of CDOM at depths shallower than 200 m. These results have important implications for enhancing our understanding of the dynamics of CDOM and DOC in east Antarctica, as well as for improving assessments of the carbon cycle.

Key words chromophoric dissolved organic matter, microbial degradation, Cosmonaut Sea, Cooperation Sea, eastern Antarctica

Citation Hu Ji, Xue Siyou, Zhou Bin, Zhao Jun, Li Dong, Fan Gaojing, Yang Disong, Zhang Leilei, Zhang Haifeng, Yu Peisong, Zhang Cai, Yang Xufeng, Zhu Changfeng, Sun Weiping, Pan Jianming. 2025. Sources and distribution characteristics of chromophoric dissolved organic matter in the Cosmonaut Sea and the Cooperation Sea, Antarctica. Acta Oceanologica Sinica, 44(4): 48–62, doi: 10.1007/s13131-024-2457-z

Foundation item: The National Natural Science Foundation of China under contract Nos 42276255, 41976228, 42176227 and 42306262; the National Polar Special Program under contract Nos IRASCC 01-01-02, IRASCC 02-02-03, and IRASCC 02-02-05; the Scientific Research Fund of the Second Institute of Oceanography under contract Nos JG2211 and JG2212.
*Corresponding author, E-mail: jmpan@sio.org.cn
http://www.aosocean.com
E-mail: ocean2@hyxb.org.cn

1 Introduction

The seasonal ice zone in east Antarctica is characterized by exceptionally high biological productivity, primarily driven by processes such as sea ice melting and upwelling during the Southern Hemisphere summer. The melting of sea ice releases freshwater, resulting in the formation of a shallow mixed layer. This nutrient-rich and light-abundant environment facilitates significant phytoplankton proliferation within the euphotic zone, leading to the establishment of diverse phytoplankton communities (Williams et al., 2010). In the waters surrounding east Antarctica, these phytoplankton communities predominantly consist of *Phaeocystis antarctica*, diatoms, and cryptophytes (Li et al., 2024). Their distribution and abundance are influenced by factors including sea ice melt, nutrient availability, and light conditions (Wright et al., 2010). For example, following sea ice melt, phytoplankton may experience reduced predation pressure, resulting in primary productivity levels that range from 25% to 67% (Smetacek et al., 2004). Marine ecosystems along the eastern coast of Antarctica are impacted by various factors, such as climate change, ocean circulation patterns, and sea ice cover (Moore et al., 1999). Additionally, the high productivity and rich biodiversity observed in the East Antarctic region during the summer contribute to the global carbon cycle.

Chromophoric dissolved organic matter (CDOM) is recognized as the optically active component of dissolved organic matter (DOM) (Coble, 2007). CDOM constitutes a subset of dissolved organic carbon (DOC) and possesses light-absorbing properties that influence light penetration depth and photosynthetic productivity in aquatic environments (Nelson et al., 2004). CDOM absorbs light in the blue wavelength range, coinciding with the absorption peaks of chlorophyll and photoprotective carotenoids, thereby limiting photosynthetic processes in aquatic systems (Arrigo and Brown, 1996). Certain phytoplankton species may adapt to high CDOM environments by altering their photosynthetic pigment composition to optimize light utilization (Nelson and Siegel, 2013). Moreover, CDOM absorbs potentially harmful UVB (280–320 nm) and UVA (320–400 nm) radiation, thereby mitigating the adverse effects of elevated ultraviolet exposure on phytoplankton communities (Arrigo and Brown, 1996). CDOM also participates in photochemical reactions that generate reactive oxygen species, which can influence various chemical reactions and biological processes in marine environments (Biers et al., 2007). Consequently, CDOM not only affects phytoplankton growth but also indirectly influences the productivity of entire marine ecosystems by regulating the light environment.

Previous studies have revealed significant regional variations in the distribution of CDOM within the Southern Ocean. In the Antarctic Peninsula region, the half-lives of CDOM range from 2.1 d to 5.1 d due to photobleaching in the upper water layers, while doubling times vary from 4.9 d to 15.7 d as a result of photohumification (Ortega-Retuerta et al., 2010). This indicates that CDOM in this region exhibits highly dynamic characteristics. In the Amundsen Sea Polynya (ASP) of the Southern Ocean, the highest recorded absorbance of CDOM at 355 nm was 0.51 m^{-1} within the euphotic layer (Lee et al., 2016). This study identified the dominant phytoplankton species, *Phaeocystis antarctica*, as a significant contributor to CDOM levels. Additionally, it was noted that the net accumulation of CDOM in the surface waters of ASP was negative, indicating the labile nature of freshly produced CDOM (Chen et al., 2019). In regions of high primary productivity within the Ross Sea, the spectral absorption coefficient of CDOM was relatively low, and the proliferation of *P. antarctica* did not directly correlate with increased CDOM levels. This suggests that variations in CDOM may be related to sea ice melt or microbial degradation occurring outside the photic zone (Kieber et al., 2009). In east Antarctica, a study indicated that ice melting may both alter the spectral characteristics of CDOM in surface waters and act as a potential source of fresh, autochthonous CDOM and labile DOC (Norman et al., 2011). Highly labile DOC is further degraded and remineralized by microorganisms within the upper 200 m of Prydz Bay, east Antarctica. The newly transformed DIC and residual DOC can be preserved in the deep layer due to the stratification of the water column during the austral summer (Jiang et al., 2024).

The dynamics of CDOM within the water column of the eastern Southern Ocean remain poorly understood, particularly in the context of unstable and variable environmental conditions, such as stratification. This study presents the geographic and vertical distribution of CDOM and DOC in the open ocean regions of the Cosmonaut Sea and Cooperation Sea. We employed excitation-emission matrix spectroscopy coupled with parallel factor analysis (EEM-PARAFAC) to achieve this. Our objective is to enhance the understanding of the sources and evolution of CDOM and to identify the factors that influence the dynamics of DOC and CDOM in this region during the austral summer.

2 Methods

2.1 *Study area and sample collection*

During the austral summer of 2019, from December 8 to December 26, samples for DOC and CDOM analysis were collected in the epipelagic layers of the Cosmonaut Sea and Cooperation Sea aboard the R/V *Xuelong 2* from the Polar Research Institute of China (PRIC) (Fig. 1). According to sea ice data (Fig. S1), the study area was characterized by open ocean conditions, devoid of sea ice coverage. The sampling sites were categorized based on the prevailing water masses into two distinct areas: waters affected by the Antarctic slope current (WAA) and areas of open water (OW), with detailed information provided in

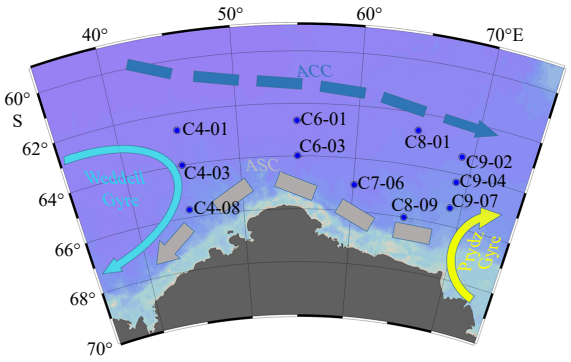


Fig. 1. Location of the stations sampled during austral summer in the 2019 cruise. The Antarctic slope current (ASC, gray), the Antarctic circumpolar current (ACC, green), the Weddell Gyre (cyan), and the Prydz Gyre (yellow) are also labeled schematically.

Table 1.

At each sampling station, parameters including pressure, salinity, and temperature were measured using a SBE 911 plus conductivity-temperature-depth (CTD) instrument equipped with a rosette sampler containing 24 Niskin bottles, each with a volume of 10 liters. The concentration of oxygen was assessed via Winkler titration, following the methodology described by Williams and Jenkinson (1982). Oxygen saturation was calculated by integrating measured data with the solubility equations established by Garcia and Gordon (1992), alongside the coefficients from Benson and Krause (1984). Apparent oxygen utilization (AOU), indicative of microbial heterotrophic metabolism, was defined as the difference between oxygen saturation and the actual concentration at a given depth, reflecting oxygen consumption throughout the study period. The mixed layer depth (MLD) was determined at the depth corresponding to the peak buoyancy frequency, in accordance with the techniques described by Carvalho et al. (2016). The index of ice-melting water (MW) was computed using the surface salinity ($S_{surface}$) and deep-water salinity (S_{deep}, approximately 300 m), following the approach outlined by Mendes et al. (2018), as expressed in Eq. (1):

$$MW = [1 - (S_{surface} - 6)/(S_{deep} - 6)] \times 100\%. \quad (1)$$

Water samples representing the characteristics of various water masses were selected at specified depths at each sampling station. For the seasonal mixed layer (SML), samples were taken from the ocean surface down to the MLD. In the WW layer, samples were obtained at the depth closest to the minimum temperature (T_{min}). For the mCDW layer, sampling was conducted at 200 m, where the average temperature was recorded at (1.51 ± 0.34)℃, with an average salinity of 34.62 ± 0.03.

2.2 *Sample treatment*

For DOC and CDOM analysis, water samples were filtered through pre-combusted Whatman GF/F filters. The resulting filtrate was distributed into two pre-combusted 20 mL glass ampoules and preserved at –20℃ for subsequent laboratory analysis.

2.3 *DOC analysis*

DOC analysis was performed using a Shimadzu TOC-L analyzer employing high-temperature combustion. Baseline measurements were established by subtracting blanks from Milli-Q water samples. The accuracy of the analyses was verified against standards (42–45 μmol C for DOC, deep sea reference from the University of Miami). Analytical errors, based on replicate measurements (with a minimum of three per sample), were maintained within 5% for DOC determinations.

2.4 *CDOM analysis*

CDOM absorbance was quantified across the ultraviolet and visible (UV-Vis) spectral range (240–800 nm) with a resolution of 1.0 nm, utilizing a Shimadzu Spectrophotometer UV-2700 and a 5 cm quartz cuvette. The absorbance (A) was converted into Napierian absorption coefficients (a) using Eq. (2):

$$a_\lambda = 2.303 \times \frac{A_\lambda}{L} + k, \quad (2)$$

where A_λ is the absorbance at the wavelength λ, L is the optical path length expressed in meter, and k is an offset calculated as the mean absorbance between wavelengths 650 nm and 700 nm (approximately zero) (Green and

Table 1. Location details in the study area

Study area	Station	Date (UTC)	Longitude/(°)	Latitude/(°)	Depth/m	MLD/m	MW/%
WAA	C4-08	2019/12/26	45.00	–65.70	3 125	23	3.6
	C8-09	2019/12/16	64.94	–66.00	3 080	14	2.9
OW	C4-01	2019/12/24	45.00	–62.65	4 605	35	3.2
	C4-03	2019/12/25	44.98	–63.99	4 276	10	2.7
	C6-03	2019/12/22	54.99	–63.98	4 490	46	3.7
	C7-06	2019/12/18	60.08	–65.00	3 949	74	3.8
	C9-04	2019/12/11	69.00	–64.32	3 205	42	2.7
	C9-07	2019/12/08	68.94	–65.32	2 764	24	2.5
	C6-01	2019/12/21	54.94	–62.64	4 825	10	3.0
	C8-01	2019/12/13	65.00	–62.65	4 169	57	3.1
	C9-02	2019/12/12	69.03	–63.32	3 825	59	3.0

Note: MLD is the mixed layer depth, MW is the index of ice-melting water.

Blough, 1994). The Napierian absorption coefficient (α_λ) was calculated at 254 nm.

Excitation emission matrices (EEMs) were obtained using a Hitachi Fluorescence Spectrofluorometer (F4700) with a 1 cm × 1 cm quartz cuvette. The excitation wavelength range was established between 250 nm and 450 nm, while the emission wavelength range spanned from 300 nm to 600 nm. Excitation scans were conducted in 5 nm increments, and emission scans were performed in 1 nm increments. Prior to analysis, corrections were made for blank subtraction, instrument bias, and Raman unit normalization. The EEM derived from Milli-Q water, measured under identical conditions, was subtracted to eliminate instrumental bias. Rayleigh and Raman scattering peaks were removed through three-dimensional interpolation (Zepp et al., 2004). EEMs were normalized to the Raman signal of water (Lawaetz and Stedmon, 2009), with fluorescence intensities expressed as equivalent water Raman Units (R.U.). Subsequently, data from the EEMs were analyzed using parallel factor analysis (PARAFAC) facilitated by the DOMFluor toolbox v1.7 (Stedmon and Bro, 2008). Model validation was achieved through visual inspection of residuals and split-half analysis. Detailed information regarding the analysis of DOC and CDOM can be found in our previous work (Hu et al., 2023).

The humification index (HIX) and the biological index (BIX), serving as indicators of the degree of humification and the contribution of biological and autochthonous dissolved organic matter (DOM), respectively, were derived from the EEMs of the samples (Huguet et al., 2009). The spectral slope ratio refers to the ratio of spectral slopes across different wavelength ranges, with a commonly used ratio being $S_{275–295}$ to $S_{350–400}$. In this study, the spectral slope ratio ($S_{275–295}$/ $S_{350–400}$, referred to as S_R) is employed as a valuable metric for differentiating between fresh, labile organic matter and aged, more complex organic matter (Helms et al., 2008). Furthermore, the specific UV absorbance at 254 nm ($SUVA_{254}$) exhibits a strong positive correlation with the percentage of aromaticity in DOC, suggesting that SUVA can effectively indicate the concentration of dissolved aromatic carbon in aquatic environments (Weishaar et al., 2003).

2.5 *Analysis of pigment concentration and identification of taxonomic groups*

Three liters of seawater for each pigment sample were filtered through a GF/F glass fiber filter (Whatman, New Castle, USA) with a gentle vacuum (<0.5 atm) and conducted under dim light conditions. The filtered samples were subsequently stored at –80℃ until laboratory analysis, which was completed within six months following the survey. The samples underwent pre-treatment as outlined by Zapata et al. (2004) prior to instrumental analysis. Three milliliter of acetone were used to extract the pigments, followed by ultrasonication in an ice bath for 30 s. The extracts were subsequently stored at –20℃ for 2 h. Then, the extract was separated from the filter debris, and the supernatant was evaporated under a gentle stream of nitrogen. The resulting residue was then re-dissolved in 300 μL of a methanol and water mixture (9:1, *v*/*v*), with analysis conducted within 4 h of preparation.

Acquity H-class ultra performance liquid chromatography (UPLC, Waters Corp., Milford, USA) was used to analyze pigment extracts, comprising UPLC-quaternary solvent manager, sample manager-FTN, PDAeλ detector, and FLR detector. The analysis employed the acquity UPLC BEH C18 column (50 mm × 2.1 mm, 1.7 μm) at a flow rate of 0.4 mL/min. A binary gradient elution program was used according to the work of Zapata et al. (2000). Pigments were qualitatively and quantitatively detected by comparing retention time, absorption spectra, and peak area in each sample chromatogram with those of authentic standards obtained from Danish Hydraulic Institute (DHI) water and environment (Hørsholm, Denmark). The detection limits and precision of the method were 2.2 μg/L and 0.26 μg/L, respectively. The CHEMTAX program (version 1.95) was used to differentiate the specific concentrations of six taxonomic groups (Feng et al., 2022).

2.6 *Statistics*

Data plotting was performed with ocean data view software (http://odv.awi.de) and Origin 9.65 software. Statistical analysis was performed with Python 3.9 software. Differences between two categories were assessed using a two-sample *t*-test, with a *p*-value threshold of 0.05 or 0.01 set to determine statistical significance.

3 Results

3.1 *Water mass and hydrographical conditions*

According to the study by Williams (2010), surface circulation in the research area is influenced by the Antarctic circumpolar current (ACC) and the Antarctic slope current (ASC), which are aligned with the full-depth circulation. In waters shallower than 250 m, circulation is primarily affected by Antarctic surface water (ASW) and modified circumpolar deep water (mCDW, see Fig. 2). ASW can be further categorized into the residual winter mixed layer, characterized by the lowest temperatures (denoted as T_{min} or winter water, WW), and SML, both of which are predominantly influenced by ice melt and solar radiation.

In the study area, sea ice began to retreat from the northeast toward the southwest starting in November 2019, resulting in only a small amount of floating ice present during the survey (see Fig. S1). In the open water (OW) region, the combined effects of ice melt and solar radiation contributed to the stratification of the water column. The MLD was measured at (18.5 ± 6.4) m in the WAA region and (39.7 ± 22.2) m in the OW region. In the WAA region, WW is primarily influenced by the ASC, leading to a broad vertical distribution (see Fig. S2), with a minimum temperature recorded at –1.82℃. However, as

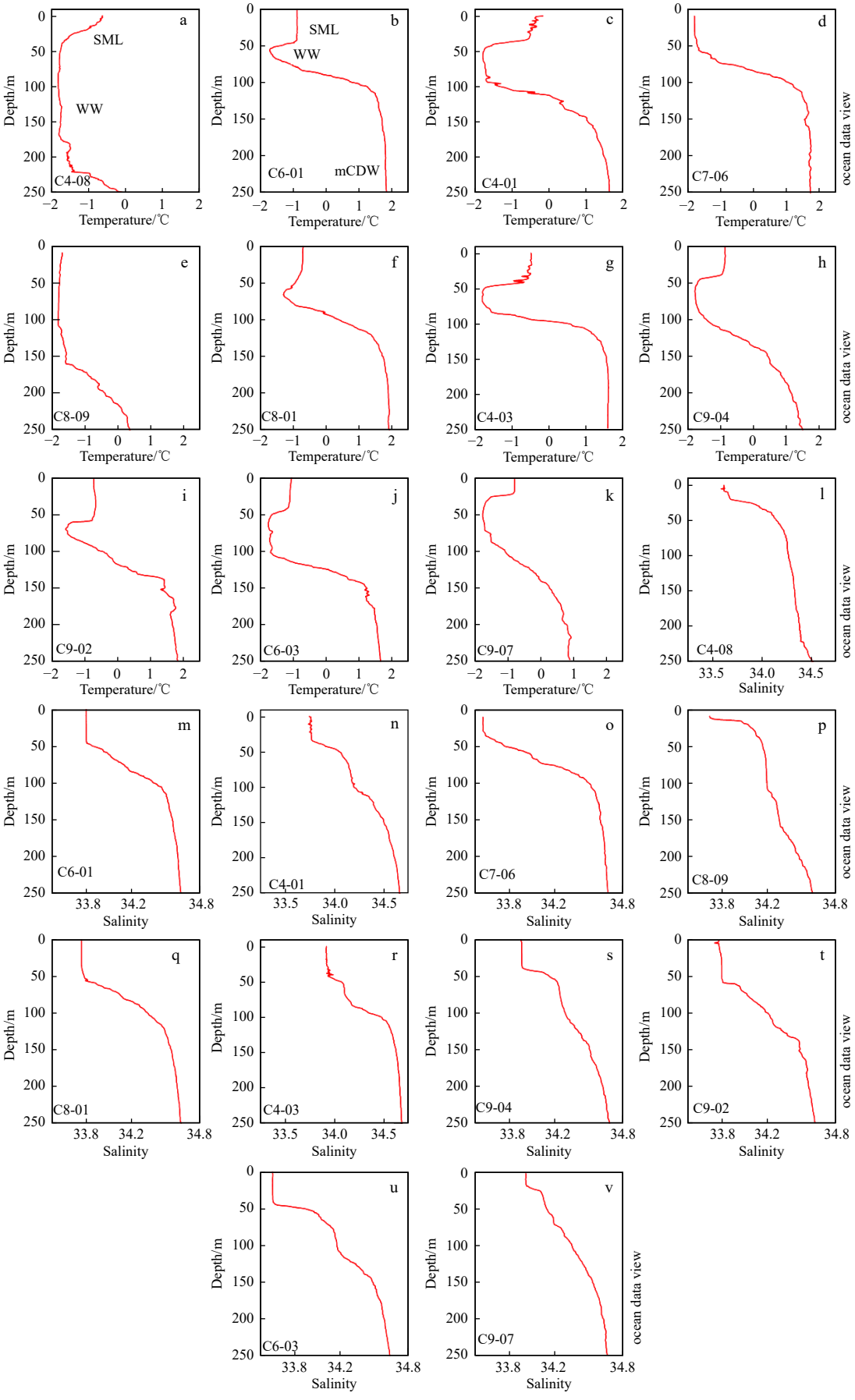


Fig. 2. The profiles of temperature (a–k) and salinity (l–v) for all stations in the epipelagic layer. The water mass identified included the seasonal mixed layer (SML), winter water (WW), and modified circumpolar deep water (mCDW).

the WW extends into the OW region, its distribution narrows due to the intrusion of warmer and saltier mCDW from below.

3.2 *Spacial distributions of Chl a, DO, and AOU*

Phytoplankton blooms were detected in the SML of the study area, with peak chlorophyll-*a* (Chl *a*) concentrations reaching 1 813.18 ng/L in the WAA region and 2 027.01 ng/L in the OW region. The mean dissolved oxygen (DO) levels were 9.82 mg/L in the WAA and 9.16 mg/L in the OW (see Table 2). The distribution of DO exhibits a similar pattern to that of Chl *a*, particularly in association with the phytoplankton bloom (refer to Fig. 3). The mean AOU values were 2.19 mg/L in the WAA and 2.53 mg/L in the OW (as shown in Table 2). Positive AOU values were recorded at all depths shallower than 200 m in both the WAA and OW regions. In the OW region, the AOU at the depth corresponding to the highest Chl *a* concentration was measured at 2.07 mg/L, indicating that microbial activity is particularly intense within the euphotic zone.

3.3 *HIX, BIX and PARAFAC components*

The mean values of HIX are 0.67 in WAA and 0.76 in OW (Table 2). Most stations recorded HIX values of less than 1.00. The mean values of BIX are 1.42 in WAA and 1.39 in OW. The HIX (<4) and BIX (>1) indices indicate a biological or aquatic bacterial origin for dissolved organic matter (DOM) (Huguet et al., 2009). The HIX value increases with water depth, whereas the BIX value shows an inverse trend (Fig. 4).

The PARAFAC method was applied in this work, and three fluorophore components were identified with our dataset (Fig. 5, Table 3). Component 1 (C1) has the exitation/emission (E_x/E_m) of 275/324 nm, and it was identified as protein-like components. The E_m of C1 is blue-shifted from authentic tryptophan fluorescence. It was reported that the fluorescence characteristics of amino acids depend on whether they are freely dissolved or bound in proteins (Lakowicz, 2006). The molecular structure changes, such as a decrease in the number of aromatic rings, reduction of conjugated bonds in a chain structure, and conversion of a linear ring system to a non-linear one,

Table 2. Mean values and ranges of environmental variables within 200 m in the study area

Area	Chl *a*/(ng·L^{-1})	DO/(mg· L^{-1})	DOC/(mg· L^{-1})	AOU/(mg· L^{-1})	a_{254}/m^{-1}	SUVA$_{254}$/(L·mg·m^{-1})	S_R	HIX	BIX
WAA	707.15	9.82	0.62	2.19	4.28	6.97	3.18	0.67	1.42
	15.10–1 813.18	7.91–11.83	0.50–0.81	–0.04–3.91	1.50–8.00	2.80–13.42	0.95–7.11	0.49–0.88	1.31–1.53
OW	581.83	9.16	0.67	2.53	5.01	7.53	2.36	0.76	1.39
	3.21–2 027.01	5.56–11.75	0.45–0.91	0.00–5.41	1.29–8.37	2.06–12.6	1.11–10.25	0.46–1.25	1.06–1.73

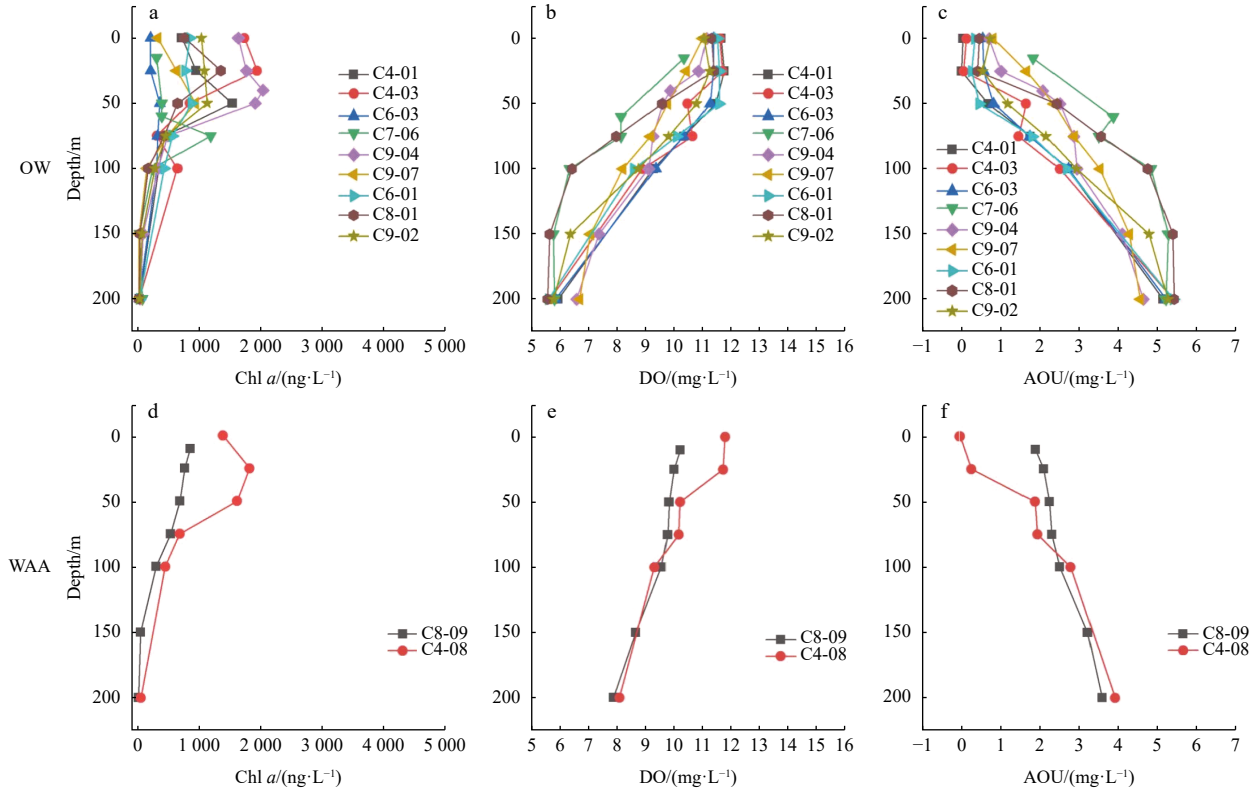


Fig. 3. Profiles of Chl *a* concentration (a and d), DO concentration (b and e), and AOU (c and f) in the research area. WAA represents waters affected by the Antarctic slope current; OW represents areas of open water.

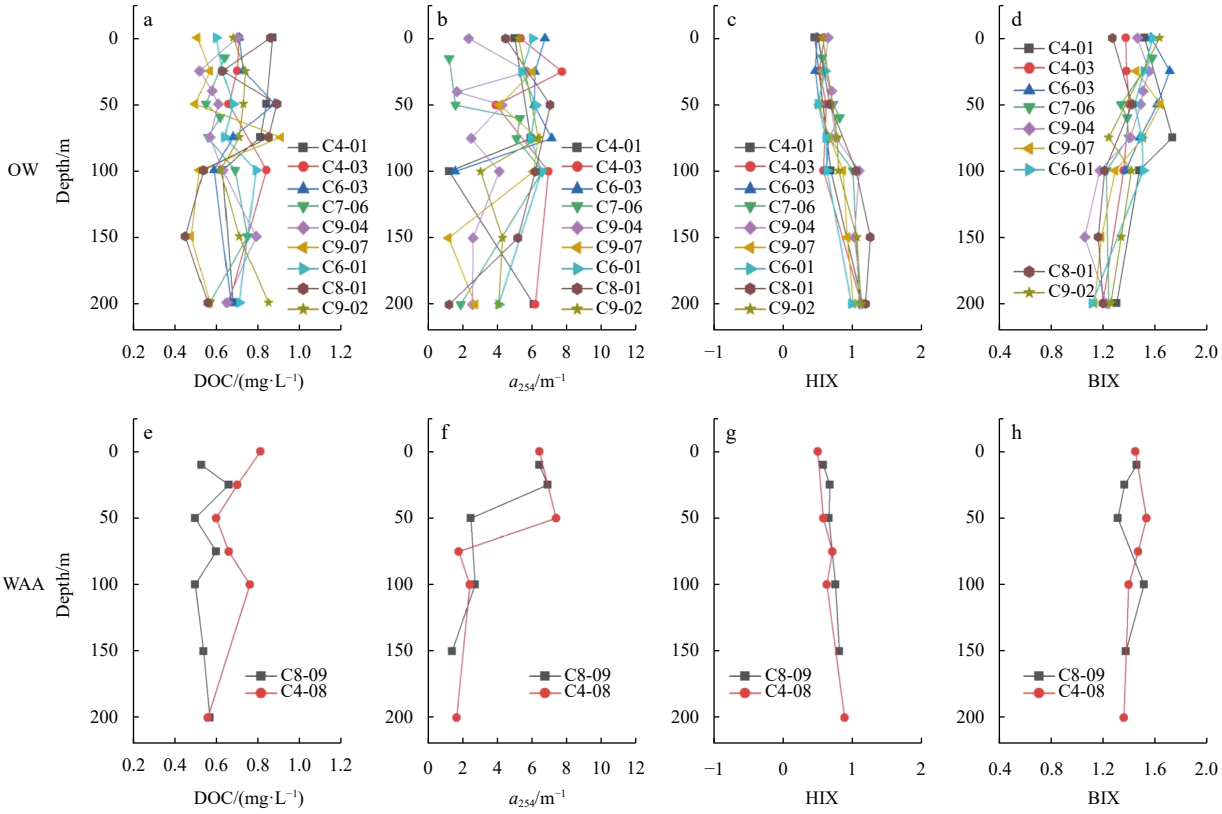


Fig. 4. The vertical distributions of DOC concentration (a and e), CDOM concentration (b and f), HIX (c and g), and BIX (d and h) in the research area.

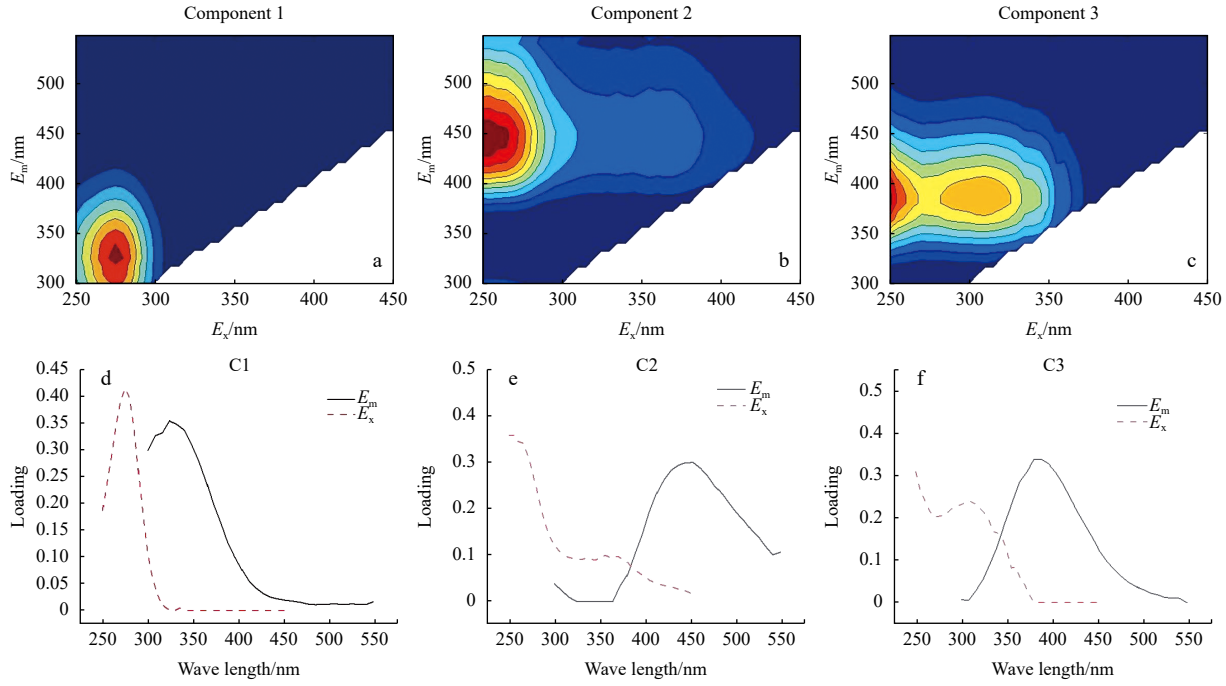


Fig. 5. EEM contour plots of the three different fluorescent components C1–C3 (a–c) identified by PARAFAC, excitation (dashed lines), and emission (solid lines) spectra of three components (d–f).

could result in blue-shift emission of CDOM (Coble, 1996). The component similar to C1 was not only reported in the coastal ocean of Ise Bay (Yamashita et al., 2008), marine sediment pore waters (Burdige et al., 2004), and ballast water in ships (Murphy et al., 2006), but also found in a highly productive Amundsen Sea Polynya (Hu et al., 2023). It is supposed to relate to the melting water from glaciers or seasonal ice. Component 2 (C2) has the primary E_x and E_m of 255 nm and 452 nm, respectively. The second E_x peak with a lesser intensity was observed

Table 3. Identification of the three PARAFAC components through the comparison with the literature data

Fluorescent component	E_x/E_m	Traditional identification	Reported literature
C1	275/324	protein-like	Burdige et al., 2004; Murphy et al., 2006; Yamashita et al., 2008
C2	255 (355) /452	UVC humic-like + UVA humic-like	Coble et al., 1996; Yamashita et al., 2003; Stedmon and Markager, 2005; Jørgensen et al., 2011
C3	(<250) 310/380	UVC humic-like + marine humic-like	Coble et al., 1996; Jørgensen et al., 2011

at the wavelength of 355 nm. C2 shows spectral characteristics similar to humic-like components (peak A + C) (Coble et al., 1998). Component 3 (C3) has a primary and secondary excitation peak, occurring around 250 nm or less and 310 nm, respectively, and a single emission peak at 380 nm. This component is characterized by absorption of UVC and UVB light. It is similar to a marine humic-like component (peak M) that occurs at E_m 370–420 nm and E_x 290–310 nm (Coble, 1996). The trend of the C1 component shows little variation with depth, while both the C2 and C3 components exhibit an increasing trend with increasing depth (Fig. 6).

4 Discussions

4.1 *Role of microbial degradation in decoupling phytoplankton crops and DOC concentrations*

The Southern Ocean is characterized by elevated phytoplankton productivity, particularly during the summer months, attributable to ample sunlight and nutrient availability. Phytoplankton contribute significantly to organic matter production through photosynthesis, which is subsequently released as DOC following phytoplankton mortality or grazing by heterotrophic organisms. Consequently, the organic matter produced by phytoplankton via photosynthesis represents a key source of DOC (Nelson et al., 1998).

In the study area, phytoplankton concentrations display a vertical gradient, with higher concentrations observed in the SML compared to the underlying WW and mCDW. However, spatial analysis reveals no significant differences in DOC distribution ($p > 0.05$, Fig. 7). For example, in the WAA, DOC concentrations in the SML do not significantly differ from those in the WW (Table S1). Similarly, in the OW, no notable differences in DOC concentrations are observed between the SML and both WW and CDW ($p > 0.05$). The results indicate that DOC concentration is statistically unrelated to Chl *a* across all ana-

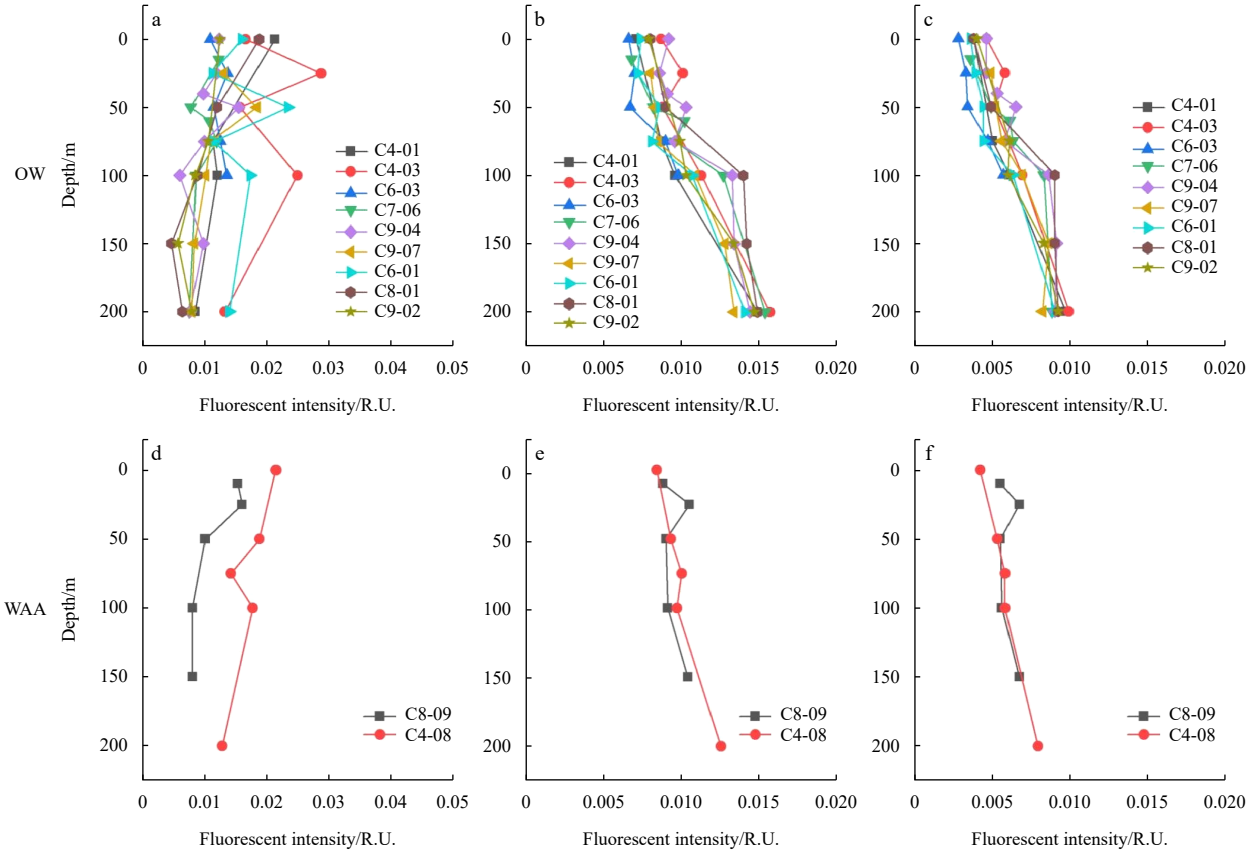


Fig. 6. Depth profiles of the EEM components C1 (a and d), C2 (b and e), and C3 (c and f) in the research area.

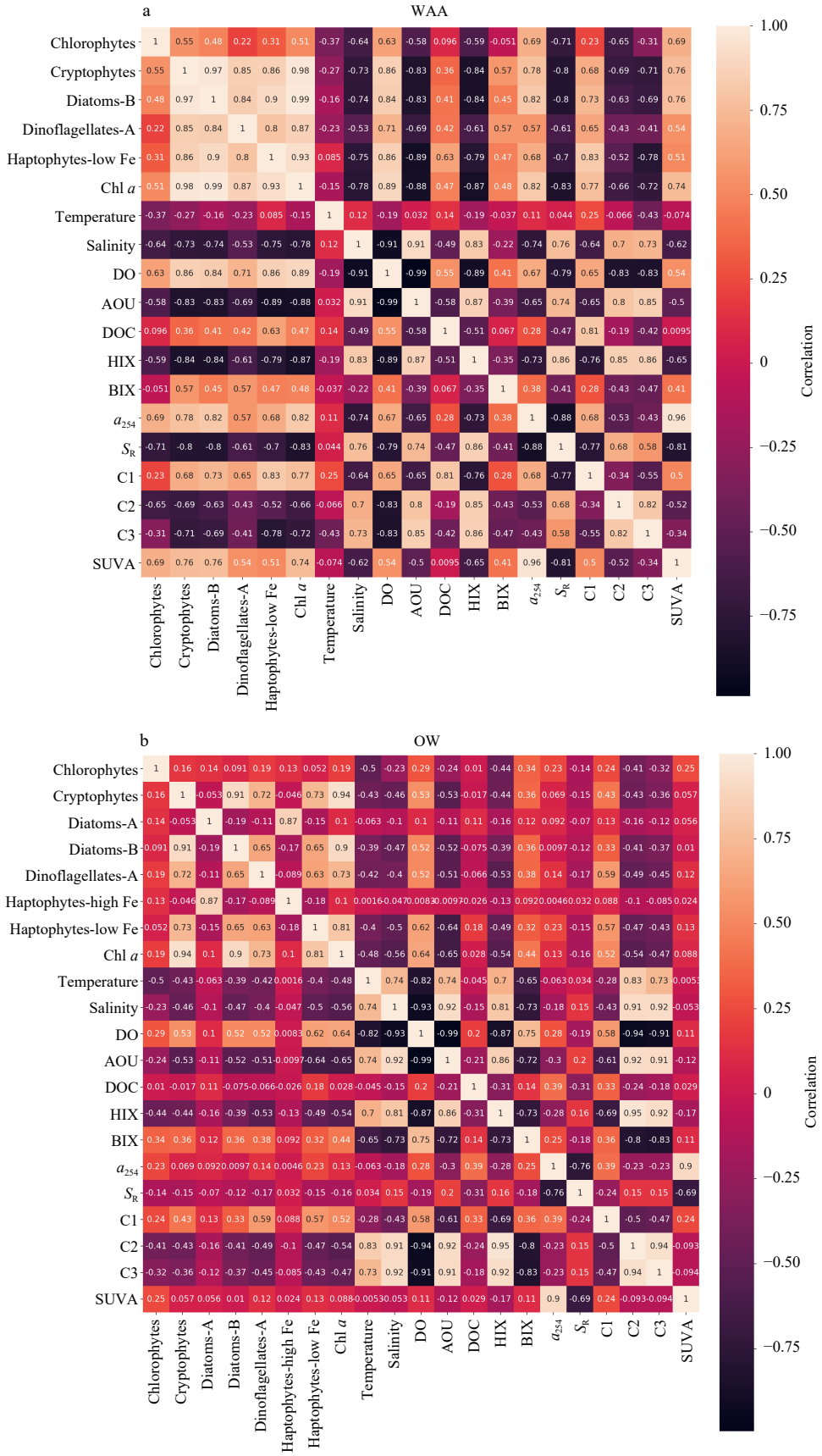


Fig. 7. The Pearson correlation coefficients of environmental variables in the study area and the corresponding heatmap (a. WAA; b. OW). The color bar represents the correspondence between colors and correlation coefficients. The colors transition from deep red (−1, representing strong negative correlation) to white (+1, representing strong positive correlation). a_{254} is the Napierian absorption coefficient which was calculated at 254 nm.

lyzed regions ($p > 0.05$, Fig. 7), suggesting that the variability in DOC concentration does not exhibit the expected correlation with chlorophyll levels.

Phytoplankton release DOC during photosynthesis, leading to increased organic carbon concentrations in the water column; thus, regions with high phytoplankton productivity typically exhibit elevated DOC concentrations (Carlson et al., 1994). However, in certain open ocean areas or specific temporal windows, a correlation between DOC and phytoplankton abundance may be absent. Several factors contribute to this lack of correlation. DOC can originate from various sources, including riverine inputs, remineralization of marine sediments, microbial degradation, and exudates from marine organisms, in addition to phytoplankton photosynthesis (Hansell and Carlson, 2001). The presence of these diverse sources complicates the relationship between DOC concentration and phytoplankton abundance. In some cases, phytoplankton growth may be limited by light or nutrient availability, such as nitrate and phosphates. For instance, subpolar and polar regions experience low temperatures and restricted light conditions, which can inhibit phytoplankton growth and obscure the relationship between DOC and phytoplankton abundance (Hansell and Carlson, 2014). Furthermore, in open ocean waters characterized by strong mixing, physical processes such as currents and vertical mixing can influence DOC distribution, further complicating its relationship with phytoplankton density (Hansell et al., 2009). In certain nutrient-poor open ocean regions, a significant correlation between DOC concentration and phytoplankton growth may be lacking (Nelson et al., 2004). In these areas, DOC primarily consists of recalcitrant organic materials whose sources and fates are less directly linked to phytoplankton productivity (Hansell and Carlson, 2014; Nelson and Siegel, 2013).

Processes such as microbial degradation, photochemical reactions, and physical mixing can all influence DOC concentrations (Hansell et al., 2009). The rapid degradation of DOC may elucidate the absence of a positive correlation between phytoplankton abundance and DOC concentration in certain areas. For example, in some regions of the Arctic and Antarctic, microbial activity may rapidly consume DOC, limiting phytoplankton access to essential nutrients and consequently affecting their population dynamics (Cherrier and Bauer, 2004).

The open waters of the Southern Ocean are situated far from land, resulting in relatively low contributions from riverine inputs and terrestrial sources of DOC, with atmospheric deposition of DOC also being minimal. Consequently, the influence of terrestrial inputs and atmospheric deposition on the distribution of DOC in the study area can be regarded as negligible. The distribution data for AOU reveal that, with the exception of a negative value at the surface of station C4-08 (–0.04 mg/L), all other water layers shallower than 200 m exhibit positive AOU values (Fig. 3). This finding indicates significant microbial metabolic activity in the upper layers, which aligns with the distribution of heterotrophic prokaryotes and phytoplankton viruses measured during the same cruise (Han et al., 2022). Therefore, we hypothesize that the intense microbial heterotrophic metabolism in the upper water layers leads to accelerated transformation rates of DOC, which is a primary factor contributing to the observed discrepancies in the spatial distribution of DOC and Chl *a*.

Microorganisms play a crucial role in the production and removal of particulate organic matter (POM) and dissolved organic matter (DOM) within marine ecosystems. Viruses facilitate the conversion of particulate organic carbon (POC) to DOM through the lysis of host cells, a process known as the "viral shunt", which influences the transformation of organic material from particulate to dissolved forms (Pearce et al., 2011). Additionally, viruses can release dissolved organic compounds through bacterial lysis, further impacting the cycling of organic matter (Fuhrman, 1999). Heterotrophic bacteria degrade DOM, converting it into inorganic forms or synthesizing new biomass, which affects the removal and transformation of DOM, thereby promoting the recycling of organic matter and the release of nutrients. Heterotrophic prokaryotes facilitate nutrient regeneration through the decomposition of organic matter (Hansell and Carlson, 2014). As summer ice melts and there is an increase in light and nutrient availability from upwelling, phytoplankton growth is enhanced, which subsequently influences the abundance of both bacteria and viruses. Microbial abundance also exhibits significant seasonal dynamics, with notable changes occurring during the ice-melting period. The growth of phytoplankton and the abundance of bacteria and viruses are temporally coupled, particularly during peak productivity periods in ice-edge ecosystems, where microbial communities also reach their highest abundances (Pearce et al., 2011).

4.2 *Relationship between phytoplankton and CDOM concentrations*

Due to limited terrestrial inputs, CDOM in the Southern Ocean is predominantly derived from biological processes occurring within the marine environment, particularly from phytoplankton production and microbial degradation (Nelson et al., 1998). However, various factors influence the relationship between CDOM and Chl *a*, which exhibits substantial variability between the WAA and the OW. In the WAA, CDOM demonstrates a positive correlation with Chl *a* and other phytoplankton pigments (Fig. 7). Among the phytoplankton community, the diatom B species shows the strongest correlation with CDOM concentration, indicating it as the primary contributor to CDOM in this region.

Existing studies have shown that in certain eutrophic areas, CDOM concentrations are positively correlated with phytoplankton crops. For example, in the phyto-

plankton communities of the Ross Sea, a correlation was observed between CDOM concentration and phytoplankton productivity (Carlson et al., 2000). This correlation primarily results from the organic matter released during phytoplankton photosynthesis, which increases CDOM concentrations in the water column. Notably, certain phytoplankton species, such as *Phaeocystis antarctica*, dominate the phytoplankton community in the Southern Ocean and significantly elevate CDOM concentrations during their bloom periods (Carlson et al., 1998). Lee et al. (2016) also identified *P. antarctica* as the main contributor to CDOM in the Amundsen Sea polynya. Thus, it is evident that there are significant spatial and temporal variations in the contribution of phytoplankton species to CDOM in the Southern Ocean, likely related to changes in phytoplankton community structure.

In contrast, the correlation between CDOM and Chl *a* is absent in the OW ($p > 0.05$). Various processes influence CDOM distribution and its relationship with phytoplankton crops in the Southern Ocean. First, light conditions in the Southern Ocean differ from those in other regions, particularly during austral summer when prolonged sunlight enhances the photodegradation of CDOM, resulting in decreased concentrations in surface waters (Andrews et al., 2000). The relatively high levels of ultraviolet (UV) radiation in this region also accelerate the photodegradation processes of CDOM, further diminishing its concentration in the upper water layers (Herndl et al., 1993). Second, strong vertical mixing in the Southern Ocean, especially within the Antarctic circumpolar current region, leads to significant mixing of surface CDOM with deeper water layers while also bringing deeper CDOM to the surface (Nelson et al., 2004).

In this study, the influence of the ASC on the WAA is notable (Fig. S2). Under the influence of the ASC, CDOM concentrations in the WW are relatively low (Table S1). However, as the WW extends northward, the influence of mCDW progressively affects water layers shallower than 200 m. Consequently, the CDOM concentration in the WW of the OW gradually increases due to the higher CDOM levels present in the SML and mCDW. Therefore, the elevated CDOM in deeper water layers due to the intrusion of CDW likely constitutes a primary reason for the absence of correlation between CDOM and Chl *a* in the OW.

A higher S_R typically indicates the presence of fresh organic material within CDOM, primarily derived from biological production by phytoplankton. Conversely, a lower S_R suggests a greater prevalence of aged organic matter, which has generally undergone microbial degradation and possesses a more complex chemical structure. In the WAA, S_R exhibits a positive correlation with salinity ($p < 0.05$, Fig. 7) but a significant negative correlation with CDOM concentration ($p < 0.01$, Fig. 7). This further confirms the substantial effects of microbial degradation in the upper water layers of this region. CDOM in both the WAA and OW demonstrates a significant positive correlation with $SUVA_{254}$ ($p < 0.01$, Fig. 7), indicating that freshly generated CDOM in the euphotic zone is characterized by relatively high aromaticity.

4.3 *Impacts of microbial heterotrophic metabolism on degradation and production of CDOM components*

In both the WAA and OW regions, the AOU values in the water column demonstrate a negative correlation with the protein-like component C1 in CDOM ($p < 0.05$, Fig. 7). This observation suggests that microbial heterotrophic metabolism is the predominant mechanism for the removal of dissolved protein-like components in the seawater of eastern Antarctica. Previous research has highlighted the critical role of the interaction between microorganisms and proteins within marine ecosystems. Microorganisms are not only essential contributors to the cycling of dissolved organic matter (DOM) and particulate organic matter (POM) in the ocean but also play significant roles in the degradation and transformation of proteins (Hansell et al., 2009).

Microbial metabolic activities are pivotal in the degradation and transformation of proteins. Studies have indicated that bacteria can effectively degrade dissolved proteins, particularly in marine environments, where the degradation rate of unprotected dissolved proteins can reach up to 92% (Borch and Kirchman, 1999). However, when proteins adsorb onto submicron particles, their degradation rates significantly decline, suggesting that the microbial utilization of proteins is influenced by environmental conditions (Keil and Kirchman, 1994). Furthermore, microorganisms facilitate protein degradation by secreting extracellular enzymes capable of breaking down complex organic materials, including proteins, thereby releasing smaller molecules such as amino acids that can be utilized by other microorganisms (Arnosti, 2011). For example, RuBisCO (ribulose-1,5-bisphosphate carboxylase/oxygenase), a protein commonly found in photosynthetic organisms, has also been identified in marine environments, underscoring its significance in microbial food webs (Orellana and Hansell, 2012). Additionally, the species composition and community structure of microorganisms significantly influence the degradation and transformation of proteins. Different bacterial communities display varying efficiencies in utilizing distinct types of proteins and amino acids, which may be linked to their metabolic pathways and ecological adaptations (Morris et al., 2010).

The relationship between CDOM and phytoplankton is indirect, with bacteria playing a crucial role in the production of CDOM (Cammack et al., 2004). Generalized additive models (GAM) can be employed to investigate the primary environmental factors influencing fluorescent components in the global ocean (Catalá et al., 2016). It was found that AOU has the most substantial impact on

Table 4. The results of power-law regression fitting in each area and comparisons with those in the global epipelagic ocean and dark global ocean

Area	C2				C3				Source
	$a/10^{-3}$	b	R^2	p	$a/10^{-3}$	b	R^2	p	
WAA	5.71 ± 0.56	0.46 ± 0.10	0.69	<0.000 1	5.82 ± 0.82	0.35 ± 0.15	0.35	<0.000 1	this work
OW	7.52 ± 0.37	0.30 ± 0.04	0.59	<0.000 1	5.93 ± 0.32	0.36 ± 0.04	0.67	<0.000 1	this work
Global epipelagic ocean	3.0 ± 0.3	0.25 ± 0.02	0.73	<0.000 1	2.9 ± 0.2	0.26 ± 0.02	0.80	<0.000 1	Catalá et al., 2016
Dark global ocean	0.09 ± 0.02	0.51 ± 0.04	0.9	<0.001 0	2.0 ± 0.4	0.31 ± 0.04	0.79	<0.001 0	Catalá et al., 2015

Note: The coefficient a represents the baseline fluorescence intensity at AOU = 1, which lacks direct biological significance. The exponent b quantifies the nonlinearity of fluorescence production/consumption rates relative to AOU variation, serving as a proxy for humic substance production efficiency.

the global distribution of humic-like components, followed by Chl *a*, exhibiting a power-law relationship. Power-law regression analysis revealed that AOU accounted for 0.69 of the variation in C2 and 0.35 in C3 in the WAA region and 0.59 of the variation in C2 and 0.67 in C3 in the OW region (Table 4). These findings corroborate that microbial heterotrophic metabolism is the principal process for the production of humic-like components in this area. Rochelle-Newall and Fisher (2002) proposed that bacteria can generate humic fluorescence through the release of non-fluorescent organic matter by phytoplankton. Numerous studies have documented a strong correlation between the production of aquatic humic-like fluorophores and microbial activity (Stedmon and Markager, 2005). Additionally, the exponential parameter (b) values for C2 and C3, derived from power-law regression analysis, were significantly higher than the mean values for the epipelagic layer of the global ocean (0.25 ± 0.02 for C2 and 0.26 ± 0.02 for C3, Catalá et al., 2016). However, these values were lower than the mean values for the global deep ocean (0.51 ± 0.04 for C2, Catalá et al., 2015). This indicates that the conversion of humic components by bacteria in the study area occurs at a rate faster than that of the epipelagic layer of the global ocean, yet slower than that of the global deep sea.

5 Conclusions

In the eastern Antarctic region, robust microbial activity in the euphotic zones of the Cosmonaut Sea and the Cooperation Sea not only represents the primary pathway for the removal of protein-like substances from the water column but also serves as a significant source of humic-like substances. Microbial degradation plays a crucial role in shaping the distribution of DOC. Furthermore, the intrusion of mCDW into the euphotic zones of these open ocean areas affects not only temperature and salinity at depths of 200 m and shallower but also the distribution of CDOM.

It is essential to consider the potential implications of increased sea ice melting on CDOM in future research. Prior studies have suggested that ice melting may produce fresh autochthonous CDOM and labile DOC, resulting in alterations to the spectral characteristics of CDOM in surface seawater (Norman et al., 2011). Therefore, it is imperative to conduct comprehensive CDOM measurements across various marine regions, particularly in polar and open ocean environments, to quantify its spatial and temporal variability. This will enhance our understanding of CDOM distribution patterns in the global ocean and its relationship with climate change. Further investigation into the biological sources of CDOM, particularly the roles of phytoplankton and microorganisms, as well as the mechanisms underlying CDOM degradation in the water column, will contribute to elucidating the interactions between CDOM and marine ecosystems.

Acknowledgement

The author thanks the Polar Research Institute of China (PRIC) and the crew of R/V *Xuelong 2* for their assistance in sample collection and analysis on board.

References

Andrews S S, Caron S, Zafiriou O C. 2000. Photochemical oxygen consumption in marine waters: A major sink for colored dissolved organic matter?. Limnology and Oceanography, 45(2): 267–277, doi: 10.4319/lo.2000.45.2.0267

Arnosti C. 2011. Microbial extracellular enzymes and the marine carbon cycle. Annual Review of Marine Science, 3: 401–425, doi: 10.1146/annurev-marine-120709-142731

Arrigo K R, Brown C W. 1996. Impact of chromophoric dissolved organic matter on UV inhibition of primary productivity in the sea. Marine Ecology Progress Series, 140: 207–216, doi: 10.3354/meps140207

Benson B B, Krause D Jr. 1984. The concentration and isotopic fractionation of oxygen dissolved in freshwater and seawater in equilibrium with the atmosphere. Limnology and Oceanography, 29(3): 620–632, doi: 10.4319/lo.1984.29.3.0620

Biers E J, Zepp R G, Moran M A. 2007. The role of nitrogen in chromophoric and fluorescent dissolved organic matter formation. Marine Chemistry, 103(1–2): 46–60, doi: 10.1016/j.marchem.2006.06.003

Borch N H, Kirchman D L. 1999. Protection of protein from bacterial degradation by submicron particles. Aquatic Microbial Ecology, 16: 265–272, doi: 10.3354/ame016265

Burdige D J, Kline S W, Chen Wenhao. 2004. Fluorescent dissolved organic matter in marine sediment pore waters. Marine Chemistry, 89(1–4): 289–311, doi: 10.1016/j.marchem.2004.02.015

Cammack W K L, Kalff J, Prairie Y T, et al. 2004. Fluorescent dissolved organic matter in lakes: Relationships with heterotrophic metabolism. Limnology and Oceanography, 49(6): 2034–2045, doi: 10.4319/lo.2004.49.6.2034

Carlson C A, Ducklow H W, Michaels A F. 1994. Annual flux of dissolved organic carbon from the euphotic zone in the northwestern Sargasso Sea. Nature, 371(6496): 405–408, doi: 10.1038/371405a0

Carlson C A, Ducklow H W, Hansell D A, et al. 1998. Organic carbon partitioning during spring phytoplankton blooms in the Ross Sea Polynya and the Sargasso Sea. Limnology and Oceanography, 43(3): 375–386, doi: 10.4319/lo.1998.43.3.0375

Carlson C A, Hansell D A, Peltzer E T, et al. 2000. Stocks and dynamics of dissolved and particulate organic matter in the southern Ross Sea, Antarctica. Deep-Sea Research Part Ⅱ: Topical Studies in Oceanography, 47(15–16): 3201–3225, doi: 10.1016/S0967-0645(00)00065-5

Carvalho F, Kohut J, Oliver M J, et al. 2016. Mixing and phytoplankton dynamics in a submarine canyon in the West Antarctic Peninsula. Journal of Geophysical Research: Oceans, 121(7): 5069–5083, doi: 10.1002/2016JC011650

Catalá T S, Álvarez-Salgado X A, Otero J, et al. 2016. Drivers of fluorescent dissolved organic matter in the global epipelagic ocean. Limnology and Oceanography, 61(3): 1101–1119, doi: 10.1002/lno.10281

Catalá T S, Reche I, Fuentes-Lema A, et al. 2015. Turnover time of fluorescent dissolved organic matter in the dark global ocean. Nature Communications, 6: 5986, doi: 10.1038/ncomms6986

Chen Meilian, Jung J, Lee Y K, et al. 2019. Production of tyrosine-like fluorescence and labile chromophoric dissolved organic matter (DOM) and low surface accumulation of low molecular weight-dominated DOM in a productive Antarctic sea. Marine Chemistry, 213: 40–48, doi: 10.1016/j.marchem.2019.04.009

Cherrier J, Bauer J E. 2004. Bacterial utilization of transient plankton-derived dissolved organic carbon and nitrogen inputs in surface ocean waters. Aquatic Microbial Ecology, 35(3): 229–241

Coble P G. 1996. Characterization of marine and terrestrial DOM in seawater using excitation-emission matrix spectroscopy. Marine Chemistry, 51(4): 325–346, doi: 10.1016/0304-4203(95)00062-3

Coble P G. 2007. Marine optical biogeochemistry: The chemistry of ocean color. Chemical Reviews, 107(2): 402–418, doi: 10.1021/cr050350+

Coble P G, Del Castillo C E, Avril B. 1998. Distribution and optical properties of CDOM in the Arabian Sea during the 1995 Southwest Monsoon. Deep-Sea Research Part Ⅱ: Topical Studies in Oceanography, 45(10–11): 2195–2223, doi: 10.1016/S0967-0645(98)00068-X

Feng Yubin, Li Dong, Zhao Jun, et al. 2022. Environmental drivers of phytoplankton crops and taxonomic composition in northeastern Antarctic Peninsula adjacent sea area. Acta Oceanologica Sinica, 41(1): 99–117, doi: 10.1007/s13131-021-1865-4

Fuhrman J A. 1999. Marine viruses and their biogeochemical and ecological effects. Nature, 399(6736): 541–548, doi: 10.1038/21119

Garcia H E, Gordon L I. 1992. Oxygen solubility in seawater: better fitting equations. Limnology and Oceanography, 37(6): 1307–1312, doi: 10.4319/lo.1992.37.6.1307

Green S A, Blough N V. 1994. Optical absorption and fluorescence properties of chromophoric dissolved organic matter in natural waters. Limnology and Oceanography, 39(8): 1903–1916, doi: 10.4319/lo.1994.39.8.1903

Han Meiaoxue, Cao Shunan, Luo Guangfu, et al. 2022. Distributions of virio- and picoplankton and their relationships with ice-melting and upwelling in the Indian Ocean sector of East Antarctica. Deep-Sea Research Part Ⅱ: Topical Studies in Oceanography, 197: 105044, doi: 10.1016/j.dsr2.2022.105044

Hansell D A, Carlson C A. 2001. Marine dissolved organic matter and the carbon cycle. Oceanography, 14(4): 41–49, doi: 10.5670/oceanog.2001.05

Hansell D A, Carlson C A. 2014. Biogeochemistry of Marine Dissolved Organic Matter. San Diego: Academic Press

Hansell D A, Carlson C A, Repeta D J, et al. 2009. Dissolved organic matter in the ocean: A controversy stimulates new insights. Oceanography, 22(4): 202–211, doi: 10.5670/oceanog.2009.109

Helms J R, Stubbins A, Ritchie J D, et al. 2008. Absorption spectral slopes and slope ratios as indicators of molecular weight, source, and photobleaching of chromophoric dissolved organic matter. Limnology and Oceanography, 53(3): 955–969, doi: 10.4319/lo.2008.53.3.0955

Herndl G J, Müller-Niklas G, Frick J. 1993. Major role of ultraviolet-B in controlling bacterioplankton growth in the surface layer of the ocean. Nature, 361(6414): 717–719, doi: 10.1038/361717a0

Hu Ji, Xue Siyou, Zhao Jun, et al. 2023. Dynamics of chromophoric dissolved organic matter in a highly productive Amundsen Sea polynya. Marine Chemistry, 257: 104329, doi: 10.1016/j.marchem.2023.104329

Huguet A, Vacher L, Relexans S, et al. 2009. Properties of fluorescent dissolved organic matter in the Gironde Estuary. Organic Geochemistry, 40(6): 706–719, doi: 10.1016/j.orggeochem.2009.03.002

Jiang Bin, Zhao Jun, Li Dong, et al. 2024. Molecular composition evolution of dissolved organic matter with water depth in Prydz Bay of East Antarctic: Carbon export implications. Journal of Geophysical Research: Oceans, 129(7): e2023JC020571, doi: 10.1029/2023JC020571

Jørgensen L, Stedmon C A, Kragh T, et al. 2011. Global trends in the fluorescence characteristics and distribution of marine dissolved organic matter. Marine Chemistry, 126(1–4): 139–148, doi: 10.1016/j.marchem.2011.05.002

Keil R G, Kirchman D L. 1994. Abiotic transformation of labile protein to refractory protein in sea water. Marine Chemistry, 45(3): 187–196, doi: 10.1016/0304-4203(94)90002-7

Kieber D J, Toole D A, Kiene R P. 2009. Chromophoric dissolved organic matter cycling during a Ross Sea phaeocycstis Antarctica bloom. In: Krupnik I, Lang M A, Miller S E, eds. Smithsonian at the Poles: Contributions to International Polar Year Science. Washington: Smithsonian Institution Scholarly Press, 319–334

Lakowicz J R. 2006. Principles of Fluorescence Spectroscopy. 3rd ed. New York: Springer

Lawaetz A J, Stedmon C A. 2009. Fluorescence intensity calibration using the Raman scatter peak of water. Applied Spectroscopy, 63(8): 936–940, doi: 10.1366/000370209788964548

Lee Y C, Park M O, Jung J, et al. 2016. Taxonomic variability of phytoplankton and relationship with production of CDOM in the polynya of the Amundsen Sea, Antarctica. Deep-Sea Research Part Ⅱ: Topical Studies in Oceanography, 123: 30–41, doi: 10.1016/j.dsr2.2015.09.002

Li Yuhong, Zhao Jun, Li Dong, et al. 2024. Factors controlling the phytoplankton crops, taxonomic composition, and particulate organic carbon stocks in the Cosmonaut Sea, East Antarctica. Journal of Oceanology and Limnology, 42(6): 1895–1908, doi: 10.1007/s00343-024-3198-6

Mendes C R B, Tavano V M, Kerr R, et al. 2018. Impact of sea ice on the structure of phytoplankton communities in the northern Antarctic Peninsula. Deep-Sea Research Part Ⅱ: Topical Studies in Oceanography, 149: 111–123, doi: 10.1016/j.dsr2.2017.12.003

Moore J K, Abbott M R, Richman J G, et al. 1999. SeaWiFS satellite ocean color data from the Southern Ocean. Geophysical Research Letters, 26(10): 1465–1468, doi: 10.1029/1999GL900242

Morris R M, Nunn B L, Frazar C, et al. 2010. Comparative metaproteomics reveals ocean-scale shifts in microbial nutrient utilization and energy transduction. The ISME Journal, 4(5): 673–685, doi: 10.1038/ismej.2010.4

Murphy K R, Ruiz G M, Dunsmuir W T M, et al. 2006. Optimized parameters for fluorescence-based verification of ballast water exchange by ships. Environmental Science & Technology, 40(7): 2357–2362

Nelson N B, Carlson C A, Steinberg D K. 2004. Production of chromophoric dissolved organic matter by Sargasso Sea microbes. Marine Chemistry, 89(1–4): 273–287, doi: 10.1016/j.marchem.2004.02.017

Nelson N B, Siegel D A. 2013. The global distribution and dynamics of chromophoric dissolved organic matter. Annual Review of Marine Science, 5: 447–476, doi: 10.1146/annurev-marine-120710-100751

Nelson N B, Siegel D A, Michaels A F. 1998. Seasonal dynamics of colored dissolved material in the Sargasso Sea. Deep-Sea Research Part Ⅰ: Oceanographic Research Papers, 45(6): 931–957, doi: 10.1016/S0967-0637(97)00106-4

Norman L, Thomas D N, Stedmon C A, et al. 2011. The characteristics of dissolved organic matter (DOM) and chromophoric dissolved organic matter (CDOM) in Antarctic sea ice. Deep-Sea Research Part Ⅱ: Topical Studies in Oceanography, 58(9–10): 1075–1091, doi: 10.1016/j.dsr2.2010.10.030

Orellana M V, Hansell D A. 2012. Ribulose-1, 5-bisphosphate carboxylase/oxygenase (RuBisCO): a long-lived protein in the deep ocean. Limnology and Oceanography, 57(3): 826–834, doi: 10.4319/lo.2012.57.3.0826

Ortega-Retuerta E, Reche I, Pulido-Villena E, et al. 2010. Distribution and photoreactivity of chromophoric dissolved organic matter in the Antarctic Peninsula (Southern Ocean). Marine Chemistry, 118(3–4): 129–139, doi: 10.1016/j.marchem.2009.11.008

Pearce I, Davidson A T, Thomson P G, et al. 2011. Marine microbial ecology in the sub-Antarctic Zone: Rates of bacterial and phytoplankton growth and grazing by heterotrophic protists. Deep Sea-Research Part Ⅱ: Topical Studies in Oceanography, 58(21–22): 2248–2259, doi: 10.1016/j.dsr2.2011.05.030

Rochelle-Newall E J, Fisher T R. 2002. Production of chromophoric dissolved organic matter fluorescence in marine and estuarine environments: an investigation into the role of phytoplankton. Marine Chemistry, 77(1): 7–21, doi: 10.1016/S0304-4203(01)00072-X

Smetacek V, Assmy P, Henjes J. 2004. The role of grazing in structuring Southern Ocean pelagic ecosystems and biogeochemical cycles. Antarctic Science, 16(4): 541–558, doi: 10.1017/S0954102004002317

Stedmon C A, Bro R. 2008. Characterizing dissolved organic matter fluorescence with parallel factor analysis: a tutorial. Limnology and Oceanography: Methods, 6(11): 572–579, doi: 10.4319/lom.2008.6.572

Stedmon C A, Markager S. 2005. Tracing the production and degradation of autochthonous fractions of dissolved organic matter by fluorescence analysis. Limnology and Oceanography, 50(5): 1415–1426, doi: 10.4319/lo.2005.50.5.1415

Weishaar J L, Aiken G R, Bergamaschi B A, et al. 2003. Evaluation of specific ultraviolet absorbance as an indicator of the chemical composition and reactivity of dissolved organic carbon. Environmental Science and Technology, 37(20): 4702–4708, doi: 10.1021/es030360x

Williams G D, Nicol S, Aoki S, et al. 2010. Surface oceanography of BROKE-West, along the Antarctic margin of the south-west Indian Ocean (30–80°E). Deep-Sea Research Part Ⅱ: Topical Studies in Oceanography, 57(9–10): 738–757, doi: 10.1016/j.dsr2.2009.04.020

Williams P J L, Jenkinson N W. 1982. A transportable microprocessor-controlled precise Winkler titration suitable for field station and shipboard use. Limnology and Oceanography, 27(3): 576–584, doi: 10.4319/lo.1982.27.3.0576

Wright S W, van den Enden R L, Pearce I, et al. 2010. Phytoplankton community structure and stocks in the Southern Ocean (30–80°E) determined by CHEMTAX analysis of

HPLC pigment signatures. Deep-Sea Research Part Ⅱ: Topical Studies in Oceanography, 57(9–10): 758–778, doi: 10.1016/j.dsr2.2009.06.015

Yamashita Y, Jaffé R, Maie N, et al. 2008. Assessing the dynamics of dissolved organic matter (DOM) in coastal environments by excitation emission matrix fluorescence and parallel factor analysis (EEM-PARAFAC). Limnology and Oceanography, 53(5): 1900–1908, doi: 10.4319/lo.2008.53.5.1900

Yamashita Y, Tanoue E. 2003. Chemical characterization of protein-like fluorophores in DOM in relation to aromatic amino acids. Marine Chemistry, 82(3–4): 255–271, doi: 10.1016/S0304-4203(03)00073-2

Zapata M, Jeffrey S W, Wright S W, et al. 2004. Photosynthetic pigments in 37 species (65 strains) of Haptophyta: implications for oceanography and chemotaxonomy. Marine Ecology Progress Series, 270: 83–102, doi: 10.3354/meps270083

Zapata M, Rodríguez F, Garrido J L. 2000. Separation of chlorophylls and carotenoids from marine phytoplankton: a new HPLC method using a reversed phase C8 column and pyridine-containing mobile phases. Marine Ecology Progress Series, 195: 29–45, doi: 10.3354/meps195029

Zepp R G, Sheldon W M, Moran M A. 2004. Dissolved organic fluorophores in southeastern US coastal waters: Correction method for eliminating Rayleigh and Raman scattering peaks in excitation-emission matrices. Marine Chemistry, 89(1–4): 15–36, doi: 10.1016/j.marchem.2004.02.006

Supplementary information:

Fig. S1. Sea ice concentration in the research area from November 2019 to January 2020. The sea ice concentration data during the cruise in Antarctica was obtained from the sea ice remote sensing system of the University of Bremen (https://seaice.uni-bremen.de/start/).

Fig. S2. Distributions of temperature (℃) along C4 transect (containing Stations C4-01, C4-03, and C4-08).

Table S1. Concentrations of DOC and CDOM in the different water masses within 200 m.

The supplementary information is available online at https://doi.org/10.1007/s13131-024-2457-z and http://www.aosocean.com/. The supplementary information is published as submitted, without typesetting or editing. The responsibility for scientific accuracy and content remains entirely with the authors.